



ChemComm

Conditional dependence of enzyme cascade reaction efficiency on the inter-enzyme distance

Journal:	<i>ChemComm</i>
Manuscript ID	CC-COM-07-2021-004162.R1
Article Type:	Communication

SCHOLARONE™
Manuscripts

COMMUNICATION

Conditional dependence of enzyme cascade reaction efficiency on the inter-enzyme distance†

Peng Lin,^a Huyen Dinh,^a Eiji Nakata,^a and Takashi Morii^{*a}

Received 00th January 20xx,
Accepted 00th January 20xx

DOI: 10.1039/x0xx00000x

A dual-enzyme cascade, xylitol dehydrogenase and xylulose kinase, derived from the xylose metabolic pathway, was constructed on a three-dimensional DNA scaffold which exhibited a dynamic shape transition from an open state to a closed hexagonal prism. Evaluation of the cascade reaction efficiencies in the open and closed states revealed little to no inter-enzyme distance dependence, presumably due to the far larger catalytic constant of the downstream enzyme. The inter-enzyme distance was not the dominant factor for cascade efficiency when the kinetic parameters of the cascade enzymes were imbalanced with the highly efficient downstream enzyme.

Cells have developed an efficient cascade reaction system to manage specific and step-by-step biochemical transformations by enzymes.^{1a} Spatially controlled organisation of cascade enzymes is observed for multi-enzyme complexes aligned on scaffolds or embedded in compartments.^{1b} One typical example is carbamoyl phosphate synthetase, which utilises a hydrophobic tunnel to overcome unfavourable enzyme kinetics and achieve a high efficiency of cascade reaction.²

While substrate channelling systems with the nature-like efficiencies are yet to be realised outside the cell, the spatial arrangements or stoichiometry of cascade enzymes have been studied to balance the velocity of each reaction in artificial metabolic pathways by applying a wide range of carriers such as proteins,³ spore surfaces,⁴ and DNA nanostructures.⁵ Among these, DNA scaffolds exhibit structural programmability and accurate addressability.⁵ The enzyme cascade efficiency has been shown to depend on the proximity of cascade enzymes on various DNA scaffolds based on the extensive studies of a pair of extremely stable enzymes, glucose oxidase (GOx) and horseradish peroxidase (HRP),^{6a-6c} where the catalytic constants (k_{cat}) of GOx and HRP are 250 s^{-1} and 33 s^{-1} , respectively (Note S1, ESI†).^{6d}

However, controversy exists whether the inter-enzyme distance indeed affects the cascade efficiency of GOx/HRP.⁷ The

proximity effect occurs only under conditions of limited time,^{7a} low concentration of intermediates,^{7b} or the presence of competing enzymes.^{7c} Zhang *et al.* proposed that catalytic enhancement of GOx/HRP resulted from the local pH decrease modulated by the negatively charged DNA scaffold surface,^{6d} but this was not applicable for the other enzymes.^{7d} By tuning the enzyme kinetic parameters of glucosidase and glucokinase using a mathematical model, Patterson *et al.* suggested that, in addition to the proximity, channelling is dependent on the kinetic balance between the two enzymes.^{7e}

Cascade enzymes in cellular metabolic reactions often suffer from unfavourable kinetics of upstream and downstream enzymes.^{1,2} The kinetic parameters of such sequential enzymes are suggested to be critical in considering the inter-enzyme distance dependence of the cascade efficiencies.⁸ Such issues will be addressed by evaluating the reaction kinetics of imbalanced cascade enzymes that are assembled with a defined inter-enzyme distance and stoichiometry on a DNA scaffold.

We studied the sequential enzymatic reaction of xylose reductase (XR) and xylitol dehydrogenase (XDH) derived from the initial step of the xylose metabolic pathway by assembling the enzymes on a 2D DNA scaffold with variations in the inter-enzyme distance.^{9a} The cascade efficiency was inversely proportional to the inter-enzyme distance.^{9a} When this XR/XDH cascade reaction was extended to the third step with xylulose kinase (XK), where k_{cat} of XK was over 200-times higher than that of XDH, the efficiency of the XR/XDH/XK cascade depended on the inter-enzyme distance of XDH and XK to a much smaller extent than that observed for the XR/XDH cascade.^{9b}

In this study, an enzyme cascade of XDH and XK (Fig. 1a) was constructed on a 3D DNA scaffold¹⁰ designed to undergo a dynamic shape transition from a pair of pyramidal dishes to a 3D hexagonal prism.¹¹ Cascade enzymes were assembled on each dish in the open state to provide an inter-enzyme distance of 60 nm. Transformation of the scaffold to the closed state resulted in an inter-enzyme distance of 20 nm while quantitatively maintaining the number of assembled enzyme molecules (Fig. 1b). Evaluation of the sequential reaction of xylitol metabolism through the transport of intermediate xylulose from XDH to XK resulted in little or no evident inter-enzyme distance dependence for the cascade reaction

^a Institute of Advanced Energy, Kyoto University, Uji, Kyoto 611-0011, Japan. Email: t-morii@iae.kyoto-u.ac.jp

† Electronic Supplementary Information (ESI) available. See DOI: 10.1039/x0xx00000x

efficiency. The results proved the conditional dependence of cascade efficiency by relying on the enzyme kinetics of upstream and downstream enzymes.

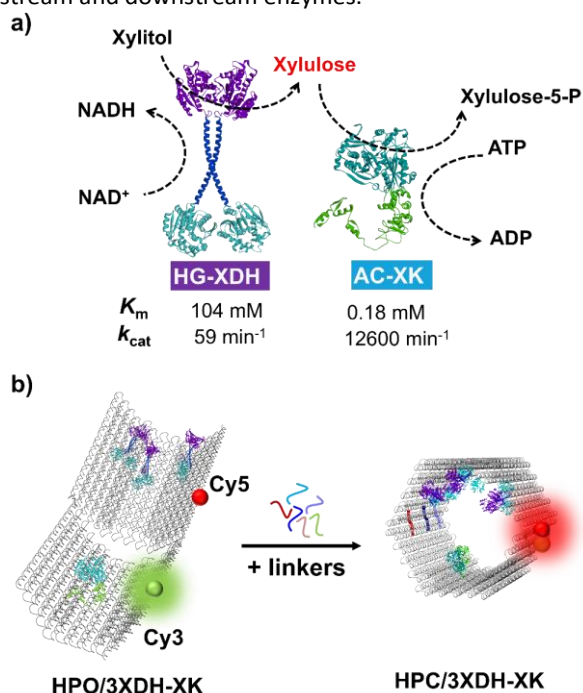


Fig. 1 (a) Schematic diagram showing the cascade reaction of HG-XDH (modular adaptor Halo-GCN4 fused XDH)^{7d} and AC-XK (modular adaptor AZ-CLIP fused XK).^{9b} The kinetic parameters are shown below each enzyme. (b) Schematic representation of the shape transformation of enzyme-loaded DNA scaffold in the open state (HPO/3XDH-XK) to its closed state (HPC/3XDH-XK) by hybridization of DNA linkers. A pair of Cy3 and Cy5 was introduced on each dish of the DNA scaffold to monitor the closing process by FRET.

The open state of the 3D DNA hexagonal prism (HP)¹⁰ consisted of a pair of truncated quadrangular pyramidal dishes with the dimensions of each dish being 17.5 nm × 35 nm × 45 nm (Fig. 1b, Fig. S1 and S2, ESI[†]).^{7d,11} Six types of single-stranded DNA linkers that hybridise with the complementary sequences spanning at both the edges of dishes were designed to fold the two dishes together in the closed state of the hexagonal prism (HPC) (Note S2, ESI[†]).¹¹ The six positions complementary to the linker sequences were left unhybridised for the open state (HPO) of the scaffold (Fig. S2, ESI[†]). A pair of donor fluorophore (Cy3) and acceptor fluorophore (Cy5) was attached at the edge of each dish of the DNA scaffold to monitor the shape transformation by changes in fluorescence resonance energy transfer (FRET). The theoretical distance between Cy3 and Cy5 was 25 nm in the fully open state and within 1 nm in the closed state (Fig. 1b).¹¹

XDH^{12a} and XK^{12b} obtained from the yeasts, *Pichia stipitis* and *Saccharomyces cerevisiae* respectively, were chosen to build a xylitol metabolic pathway on the DNA scaffold (Fig. 1). Modular adaptors^{9,13} consisting of the sequence-specific DNA binding protein and the self-ligating protein-tag were used to stably locate the enzymes at specific positions on the DNA scaffold with a covalent linkage between the protein-tag and DNA scaffold. The modular adaptor-fused upstream enzyme HG-XDH (Halo-GCN4 fused XDH) and the second enzyme AC-XK (AZ-CLIP

fused XK) were constructed as reported previously (Fig. 1a and Fig. S3, ESI[†]).^{7d,9b} Three hairpin DNAs with the target DNA sequences modified with 5-chlorohexane (CH) for HG-XDH and/or single hairpin DNA with the target DNA sequence modified with benzylguanine (BC) for AC-XK were located on each of the truncated quadrangular pyramidal dishes of the DNA scaffold in the open state.

The DNA scaffolds with modular adaptor binding sites in the open state were incubated with HG-XDH and/or AC-XK at 4 °C for 1 h. The binding mixtures were purified by gel filtration to remove the unbound proteins to give purified DNA-enzyme assemblies: enzymes co-assembled on the open state (HPO/3XDH-XK), individually loaded XDH on the open state (HPO/3XDH), or individually loaded XK on the open state (HPO/XK) (Fig. 2a). The loading yield of the enzyme on each DNA scaffold was quantitated by atomic force microscopy (AFM) images (Fig. 2b and Table S1, ESI[†]).^{7d} HG-XDH was deformed during AFM analysis to locate the plausible XDH domain outside the DNA scaffold (Fig. S4, ESI[†]).^{7d} On average, 2.47 ± 0.11 molecules of HG-XDH (dimer) and 0.67 ± 0.06 molecules of AC-XK (monomer) were loaded on each DNA scaffold for HPO/3XDH-XK (Fig. S4, ESI[†]), 2.53 ± 0.10 molecules of HG-XDH (dimer) on each HPO/3XDH (Fig. S5, ESI[†]), and 0.91 ± 0.02 molecules of AC-XK (monomer) on HPO/XK (Fig. S6, ESI[†]). Note that the loading yield of AC-XK for the co-assembled system was lower than that of the individually assembled system. This was presumably caused by the steric hindrance between HG-XDH (16 × 9 nm) and AC-XK (10 × 8 nm) (Fig. S3, ESI[†]).

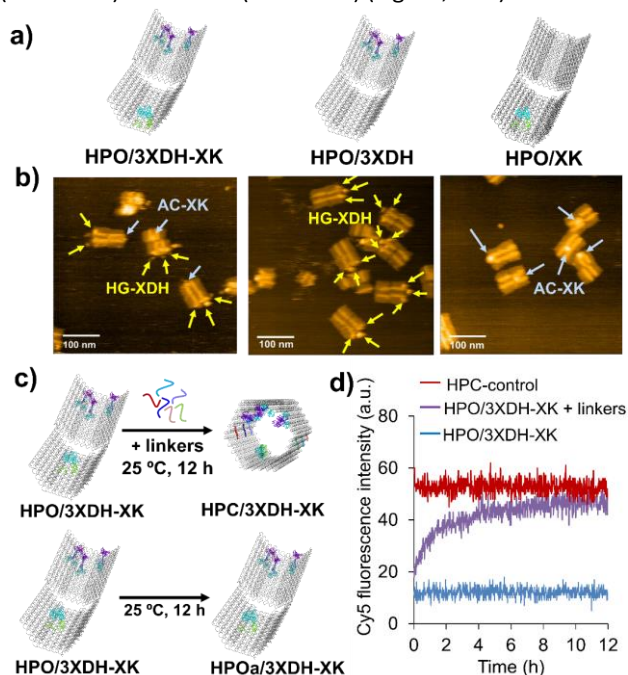


Fig. 2 (a) Illustrations of HPO/3XDH-XK, HPO/3XDH and HPO/XK. (b) Typical AFM images of HPO/3XDH-XK (left), HPO/3XDH (middle) and HPO/XK (right) (scale bar: 100 nm). The arrows in yellow and blue indicated the assembled HG-XDH and AC-XK, respectively. (c) HPO/3XDH-XK was incubated in the presence or the absence of DNA linkers to obtain HPC/3XDH-XK or HPOa/3XDH-XK (the control sample treated with the same incubation conditions). (d) Time course changes of Cy5 fluorescence intensity ($\lambda_{em} = 670$ nm) during the incubation of HPO/3XDH-XK in the presence (purple) or absence (blue) of DNA linkers upon the excitation of Cy3 at 520 nm. A pre-formed HPC was used as HPC-control (red) for the FRET measurement.

After assembly of enzymes on the DNA scaffold in an open state, each assembly—HPO/3XDH-XK, HPO/3XDH, or HPO/XK—was incubated in the presence of DNA linkers at a molar ratio of 1:1 to transform to a closed state encapsulating the enzymes (HPC/3XDH-XK, HPC/3XDH, and HPC/XK). HPOa/3XDH-XK, HPOa/3XDH, and HPOa/XK denote control samples of the enzyme assemblies in the open state treated under the same incubation process for the above shape transformation in the absence of DNA linkers (Fig. 2c and Fig. S7, ESI[†]). The time course of the closing process for the DNA scaffold assembled with enzymes was monitored using the Cy5 fluorescence intensity to yield an over 90% closed structure after the incubation for 12 h (Fig. 2d and Fig. S8, ESI[†]).¹¹ Formation of the closed structures was further verified by their AFM images, in which the closed state of HPO/3XDH-XK was observed in over 95% yield (Fig. S9, ESI[†]). These results indicate that the HPO scaffold was efficiently transformed into the HPC scaffold by encapsulating the assembled enzymes.

Enzyme cascade reactions in the open and closed states were investigated for the co-assembled systems (HPOa/3XDH-XK or HPC/3XDH-XK), and an equimolar mixture of enzymes individually loaded in an open or closed system (HPOa/3XDH + HPOa/XK or HPC/3XDH + HPC/XK). In the XDH/XK cascade reaction, the first enzyme HG-XDH converted xylitol into xylulose by consuming the cofactor NAD⁺, and the second enzyme AC-XK phosphorylated the resulting xylulose into xylulose-5-phosphate by consuming ATP (Fig. 1a). The activity of HG-XDH on each DNA scaffold was measured by monitoring the time-dependent changes in absorbance at 340 nm, indicating NADH production (Fig. 3a and Fig. S10, ESI[†]). The comparable initial reaction velocity of HG-XDH for different reaction systems further supported that the loading yields of HG-XDH on DNA scaffolds were similar (Fig. 3b and Table S1, ESI[†]).

The cascade reaction of XDH and XK was analysed by high performance liquid chromatography (HPLC) to quantitate adenosine diphosphate (ADP) generated in the reactions at steady state after 24 h (Fig. 3c and Fig. S11, ESI[†]). Notably, NADH was decomposed when enzyme reactions were quenched by the addition of trifluoroacetic acid (TFA) (to 0.1% TFA) (Note S3 and Fig. S12, ESI[†]).¹⁴ The amount of ADP produced by the second enzyme AC-XK was used to measure the efficiency of the XDH/XK cascade reaction. Comparison of the HPOa/3XDH-XK and HPC/3XDH-XK systems, which share the same assembly yield of HG-XDH and AC-XK, revealed insignificant enhancement of ADP production in the closed state over the open state, despite the difference in the inter-enzyme distance between XDH and XK. The individually assembled systems displayed ADP production yields similar to the co-assembled systems, which was due to the higher AC-XK loading yield for HPOa/XK and HPC/XK mentioned above (Fig. 3d and Table S1, ESI[†]).

To directly compare the enzyme cascade reaction efficiencies of these reaction systems, the turnover number for each reaction system was obtained from the amount of produced ADP normalised by the concentration of the second enzyme AC-XK on the DNA scaffold in the time unit (24 h) (Note

S4, ESI[†]). The turnover numbers of HPC/3XDH-XK and HPOa/3XDH-XK were comparable, while the equimolar mixture of individually loaded systems (HPOa/3XDH + HPOa/XK or HPC/3XDH + HPC/XK) revealed lower turnover numbers than the co-assembly (Fig. 4a).

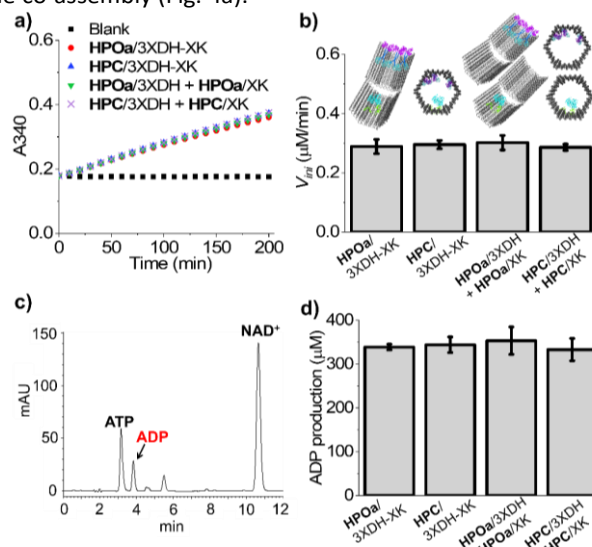


Fig. 3 (a) Time course changes of the absorbance at 340 nm (A340) for the enzyme cascade reactions on the DNA scaffold. (b) Comparison of the initial reaction velocities of HG-XDH in the enzyme cascade reactions on the DNA scaffold obtained from (a). (c) HPLC chromatograph for the reaction products by enzyme cascade HPC/3XDH-XK after 24 h. (d) ADP production (μM) of the enzyme cascade reactions on the DNA scaffold quantitated by HPLC. Conditions for the cascade reaction are indicated in Fig. S11.

The inter-enzyme distances of XDH and XK for HPOa/3XDH-XK in the fully open state and HPC/3XDH-XK were estimated to be approximately 60 nm and 20 nm, respectively (Fig. S13, ESI[†]). The inter-enzyme distance of XDH and XK in the mixture of individually loaded XDH and XK was estimated to be 1110 nm based on the concentration of the DNA scaffold (Note S5, ESI[†]). From the plot of turnover number against inter-enzyme distance, no evident distance dependence was observed for the cascade reaction of XDH/XK (Fig. 4b). The plot shows a marked contrast to the one obtained from the enzyme pair XR/XDH co-assembled on a 2D DNA scaffold in our previous study (Fig. 4c, Fig. 4d, and Fig. S14, ESI[†]).^{9a}

The Michaelis constants (K_m) of HG-XDH and AC-XK for xylitol and xylulose are 104 mM and 0.18 mM, respectively.^{9b} The turnover numbers (k_{cat}) of HG-XDH and AC-XK are 59 min⁻¹ and 12600 min⁻¹, respectively (Fig. 1a and Table S2, ESI[†]).^{9b} Although XDH/XK cascade reactions were performed with the controlled stoichiometry of 6:1 for HG-XDH (monomer) to AC-XK (monomer), the variation of the inter-enzyme distance from 60 nm to 20 nm on the DNA scaffold was not sufficient to mark an evident distance dependence, possibly due to the far larger k_{cat} and lower K_m of the second enzyme AC-XK. In the XR/XDH cascade, K_m (for xylose) and k_{cat} of ZS-XR (ZF-SNAP fused XR)^{9a} were 256 mM and 125 min⁻¹, respectively (Table S2, ESI[†]). The kinetic parameters for the enzymes in the XR/XDH cascade are much more balanced than those for the XDH/XK cascade, which likely elicited the sharper inter-enzyme distance dependence of the XR/XDH cascade efficiency (Fig. 4d).^{9a}

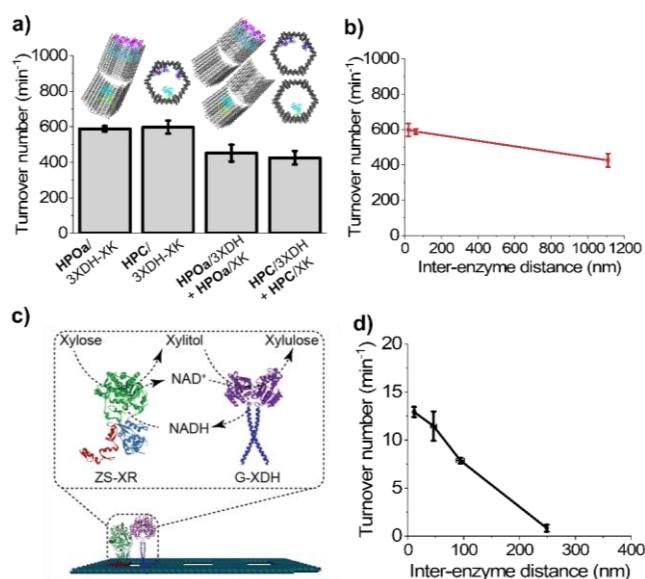


Fig. 4 (a) Turnover numbers of the enzyme cascade reactions of HG-XDH and AC-XK. (b) The plot of turnover number versus inter-enzyme distance of HG-XDH and AC-XK on the DNA scaffold. (c) Schematic representation of the ZS-XR/G-XDH enzyme cascade reaction on a 2D DNA scaffold; G-XDH denoted adaptor GCN4-fused XDH.^{9a} (d) The plot of turnover number of ZS-XR/G-XDH assembled on a 2D DNA scaffold versus inter-enzyme distance of ZS-XR and G-XDH. The enzyme cascade reaction conditions are indicated in Fig. S14.^{9a}

The effect of enzyme kinetics on the overall enzyme cascade efficiency was studied by Hess *et al.*¹⁵ Based on the kinetic simulation of the enzyme cascade GOx/HRP, they proposed that the downstream enzyme is not the rate-limiting step when the downstream enzyme has a lower K_m value and a much higher k_{cat} than the upstream enzyme.^{15a} In a sequential cascade with different maximum rates for the first and second enzymes, the output converges to the maximum rate of the slower enzyme.^{15b} In the case of the XDH/XK cascade, the second enzyme XK displays a much larger k_{cat} and lower K_m than the upstream enzyme XDH. The experimental conditions in the presence of excess ATP provided a unimolecular transfer system, where only the intermediate xylulose produced by XDH accounts for the XK reaction. Such conditions provided a similar overall output despite the variation in the inter-enzyme distance from 60 nm to 20 nm for XDH and XK.

In summary, the enzyme cascade XDH/XK was assembled on a 3D DNA scaffold with efficient dynamic shape transformation, which can be applied for the construction of an artificial metabolic pathway. The inter-enzyme distance was varied from 60 nm to 20 nm via transition from the open state to the closed state of a DNA hexagonal prism. The enzymes co-encapsulated in the closed state displayed a cascade efficiency comparable to that of co-assembled enzymes in the open state. Our results indicate that the inter-enzyme distance is not the dominant factor for the cascade reaction, for which the kinetic parameters of the cascade enzymes are imbalanced with the highly active downstream enzyme. This assumption provides insights into the spatial design of enzymes involved in the artificial metabolic pathway.

This work was supported by JSPS KAKENHI Grant Numbers 17H01213 (T.M.) and JST CREST Grant Number JPMJCR18H5

(T.M.), Japan. Peng Lin would like to acknowledge the China Scholarship Council (CSC) for the PhD scholarship.

Conflicts of interest

There are no conflicts to declare.

Notes and references

- (a) I. Wheeldon, S. D. Minter, S. Banta, S. C. Barton, P. Atanassov and M. Sigman, *Nat. Chem.*, 2016, **8**, 299-309. (b) R. J. Conrado, J. D. Varner and M. P. DeLisa, *Curr. Opin. Biotechnol.*, 2008, **19**, 492-499.
- E. W. Miles, S. Rhee and D. R. Davies, *J. Biol. Chem.*, 1999, **274**, 12193-12196.
- J. E. Dueber, G. C. Wu, G. R. Malmirchegini, T. S. Moon, C. J. Petzold, A. V. Ullal, K. L. Prather and J. D. Keasling, *Nat. Biotechnol.*, 2009, **27**, 753-759.
- L. Chen, A. Mulchandani and X. Ge, *Biotechnol. Prog.*, 2017, **33**, 383-389.
- F. Hong, F. Zhang, Y. Liu and H. Yan, *Chem. Rev.*, 2017, **117**, 12584-12640.
- (a) J. Fu, M. Liu, Y. Liu, N. W. Woodbury and H. Yan, *J. Am. Chem. Soc.*, 2012, **134**, 5516-5519. (b) L. Xin, C. Zhou, Z. Yang and D. Liu, *Small*, 2013, **9**, 3088-3091. (c) O. I. Wilner, Y. Weizmann, R. Gill, O. Lioubashevski, R. Freeman and I. Willner, *Nat. Nanotechnol.*, 2009, **4**, 249-254. (d) Y. Zhang, S. Tsitkov and H. Hess, *Nat. Commun.*, 2016, **7**, 1-9.
- (a) O. Idan and H. Hess, *ACS Nano*, 2013, **7**, 8658-8665. (b) A. Kuzmak, S. Carmali, E. von Lieres, A. J. Russell and S. Kondrat, *Sci. Rep.*, 2019, **9**, 1-7. (c) Y. Cao, X. Li, J. Xiong, L. Wang, L. T. Yan and J. Ge, *Nanoscale*, 2019, **11**, 22108-22117. (d) P. Lin, H. Dinh, Y. Morita, Z. Zhang, E. Nakata, M. Kinoshita and T. Morii, *Chem. Commun.*, 2021, **57**, 3925-3928. (e) D. P. Patterson, B. Schwarz, R. S. Waters, T. Gedeon and T. Douglas, *ACS Chem. Biol.*, 2014, **9**, 359-365.
- F. Hinzpeter, U. Gerland and F. Tostevin, *Biophys. J.*, 2017, **112**, 767-779.
- (a) T. A. Ngo, E. Nakata, M. Saimura and T. Morii, *J. Am. Chem. Soc.*, 2016, **138**, 3012-3021. (b) T. M. Nguyen, E. Nakata, M. Saimura, H. Dinh and T. Morii, *J. Am. Chem. Soc.*, 2017, **139**, 8487-8496.
- S. M. Douglas, I. Bachelet and G. M. Church, *Science*, 2012, **335**, 831-834.
- P. Lin, H. Dinh, E. Nakata and T. Morii, *Front. Chem.*, 2021, **9**, 697857.
- (a) S. Watanabe, T. Kodaki, and K. Makino, *J. Biol. Chem.*, 2005, **280**, 10340-10349. (b) S. L. Pival, R. Birner-Gruenberger, C. Krump and B. Nidetzky, *Protein Expr. Purif.*, 2011, **79**, 223.
- (a) E. Nakata, H. Dinh, T. A. Ngo, M. Saimura and T. Morii, *Chem. Commun.*, 2015, **51**, 1016-1019. (b) T. M. Nguyen, E. Nakata, Z. Zhang, M. Saimura, H. Dinh and T. Morii, *Chem. Sci.*, 2019, **10**, 9315-9325.
- K. A. J. Walsh, R. M. Daniel and H. W. Morgan, *Biochem. J.*, 1983, **209**, 427-433.
- (a) Y. Zhang and H. Hess, *ACS Catal.*, 2017, **7**, 6018-6027. (b) S. Tsitkov, T. Pesenti, H. Palacci, J. Blanchet and H. Hess, *ACS Catal.*, 2018, **8**, 10721-10731.